Applications of Frequency Domain Curve-fitting in the EFDD Technique

Niels-Jørgen Jacobsen
Brüel & Kjær Sound & Vibration Measurement A/S
Skodsborgvej 307, DK-2850 Nærum, Denmark

Palle Andersen
Structural Vibration Solutions A/S
NOVI Science Park, Niels Jerners Vej 10, DK-9220 Aalborg East, Denmark

Rune Brincker
Department of Civil Engineering, University of Aalborg
Sohngaardsholmsvej 57, DK-9000 Aalborg, Denmark

ABSTRACT

Over the years different methods have been proposed for how to deal with the presence of harmonic components in operational modal analysis. In this paper a method for detection of harmonic components using Fast Kurtosis Checking will be introduced along with a new frequency domain curve-fitting version of the Enhanced Frequency Domain Decomposition (EFDD) technique. This combined approach makes it possible to extract structural modes fast even when several harmonic components are present and even when the harmonic components are located exactly at the natural frequencies of the structural modes. The applicability of the combined approach is assessed for a case within mechanical engineering as well as a case within civil engineering.

1   INTRODUCTION

The algorithms used in Operational Modal Analysis assume that the input forces to the structure under test are stochastic in nature. The loading forces of many structures are, however, often more complex with significant harmonic components (deterministic signals) superimposed on the stochastic broadband excitation. As the input forces are not measured in Operational Modal Analysis, special attention must be paid to identify and separate the harmonic components from the true structural modes and to reduce their influence in the modal parameter extraction process. As described in Jacobsen [1], the consequences of having stochastic signals superimposed by harmonic components can be quite severe and can significantly bias the modal parameters obtained or even prohibit the extraction of the structural modes.

In Jacobsen [1] various easy-to-use methods for identifying harmonic components and structural modes were also investigated. This included the Short Time Fourier Transform (STFT), Singular Value Decomposition (SVD), Visual Mode Shape Comparison, Modal Assurance Criterion (MAC), Stabilization Diagram and Probability Density Functions (PDFs). Despite being very powerful in the cases of well-separated structural modes and harmonic components, the methods were not very suitable for a robust automated method for separating closely-coupled structural modes and harmonic components.

In Jacobsen et al. [2] a robust automated harmonic indicator based on kurtosis calculations was introduced. The paper also described how the harmonic components were eliminated by linear interpolation in the SDOF functions derived using the EFDD technique, i.e. without using potentially destructive filtering. The method gave good results but could be optimized as regards computational efficiency and accuracy when a harmonic component was located exactly at the peak of a structural mode.

In this paper, a significantly faster version of the harmonic indicator will be presented. Instead of checking the responses at all frequencies in every measurement channel, this new harmonic indicator works by only performing the check in a selected number of measurement channels (projection channels) and only for frequencies, where there is an abrupt change in the Singular Value Decomposition (SVD) curves of the response spectral density matrix. An abrupt change indicates a potential harmonic component that has to be further investigated. Having detected the harmonic components, their influence are significantly reduced by applying a curve-fitting version of the EFDD technique giving a more accurate estimation of the natural frequencies and damping ratios.

The applicability of the new combined approach is discussed and applied to two real cases within mechanical engineering and civil engineering – a ship structure and a gravity dam.

2 IDENTIFICATION OF HARMONIC COMPONENTS

2.1 EXTENDED KURTOSIS CHECKING

In Jacobsen et al. [2] an Extended Kurtosis Checking method was described and shown to be a robust harmonic indicator. It was based on various applications of kurtosis calculations. The kurtosis γ of a stochastic variable x provides a way of expressing how peaked or how flat the probability density function of x is. The kurtosis is defined as the fourth central moment of the stochastic variable normalized with respect to the standard deviation σ as follows:

$$\gamma(x|\mu,\sigma) = \frac{E\left[(x-\mu)^4\right]}{\sigma^4} \tag{1}$$

where μ is the mean value of x and E is denoting the expectation value.

The PDF of the response of a pure structural mode will be normally distributed with a kurtosis $\gamma = 3$, whereas the kurtosis $\gamma = 1\frac{1}{2}$ for a sinusoidal component.

The output of the Extended Kurtosis Checking method is a Harmonic Indicator H_j defined for each frequency from DC to the Nyquist frequency. It returns the value 1 in case of a harmonic component and otherwise 0.

The steps in the automated Extended Kurtosis Checking method are roughly as follows:
1. Each measurement channel y_i is normalized to zero mean and unit variance.
2. For all frequencies f_j from DC to the Nyquist frequency a narrow bandpass filtering of y_i around f_j is performed.
3. The Kurtosis $\gamma_{j,i}$ for the filtered signal y_i around f_j is calculated.
4. For each frequency f_j, the mean of the Kurtosis γ_j is calculated across all the measurement channels.
5. The median m of the Kurtosis of all frequencies is calculated. If the signal is purely Gaussian distributed this robust measure for the mean will theoretically be 3 (equation (1)).
6. For each frequency f_j the deviation of the Kurtosis γ_j from the median m is calculated. If γ_j deviates significantly from m, then the distribution around f_j is different than for the majority of the other frequencies. In such a case the signals at f_j can be characterized as outliers and should not be included in the estimation of the SDOF functions. Hence the harmonic indicator H_j is set equal to 1. Otherwise H_j is set equal to 0.
7. The harmonic indicator Hj is automatically plotted as vertical lines in the SVD plot of the response spectral density matrix.

As the method is quite computational intensive, it becomes rather time consuming in case of measurements performed in many channels analyzed using a high number of frequency lines.

Figure 1 below shows the result of the Extended Kurtosis Check method applied to the responses of an aluminum plate structure excited with randomly spaced broadband stochastic excitation and a single-point sinusoidal signal at 374 Hz with 2nd and 4th harmonics at 748 Hz and 1496 Hz, respectively. The harmonic components are clearly found and indicated as vertical lines.
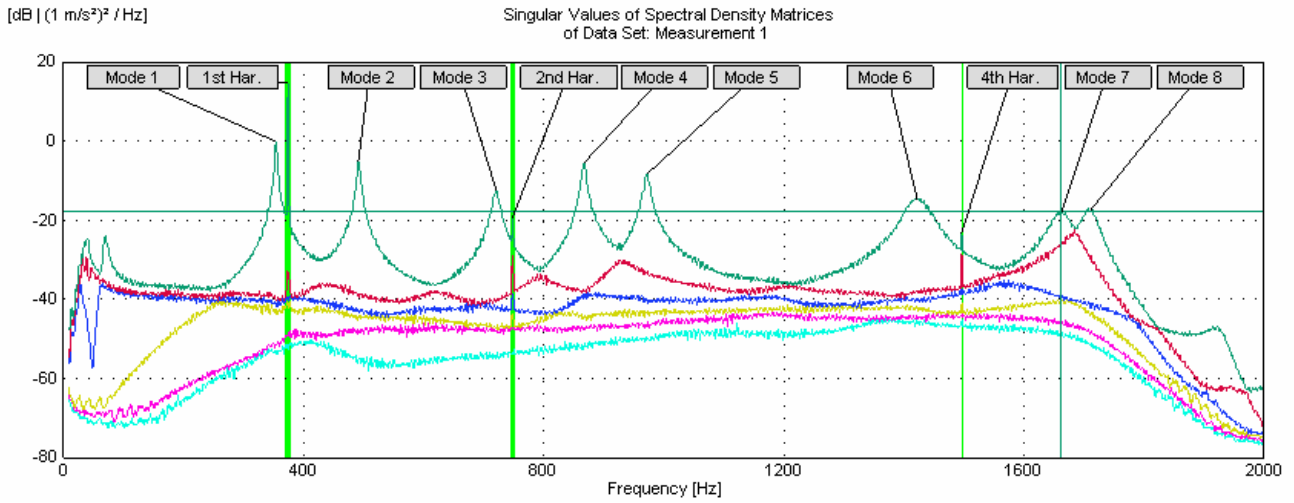
Figure 1. Indication of structural modes and harmonic components in the SVD plot.
Harmonic components at 374 Hz, 748 Hz and 1496 Hz (vertical green lines).

2.2 FAST KURTOSIS CHECKING

In Andersen et al. [3] an alternative method is proposed using fewer measurement channels and frequency lines. The method is referred to as the Fast Kurtosis Checking method.

2.2.1 REDUCING THE NUMBER OF MEASUREMENT CHANNELS

For a system with many measurement channels n_y, the spectral density matrix $G_{yy}(f)$ of the measured responses typically consist of much more rows/columns than there are structural modes. Many of the rows/columns are linear dependent resulting in a rank deficiency of the spectral matrix $G_{yy}(f)$. For such a system there is consequently a substantial amount of redundancy, indicating that it might not be necessary to include all of the measurement channels in the algorithm for the harmonic indicator. The subset of measurement channels to be used is called the projection channels and the number of projection channels is denoted n_p.

Selection of the projection channels is based on simple correlation analysis calculating the correlation coefficients C_{ij} between the measurement channels $y(t)$:

$$C_{ij}^2 = \frac{E\left[\left(y_i(t)y_j(t)\right)^2\right]}{E\left[y_i(t)y_i(t)\right]\,E\left[y_j(t)y_j(t)\right]} \tag{2}$$

The projection channels are automatically found using the following procedure:
1a. If the test is performed using multiple data sets and roving transducers, a good initial choice is to use the reference channels as projection channels. The reference channels correlate most with the other channels, since they are present in all data sets.
1b. If the test is performed in a single data set, find the channel i that correlates most with the other channels. This channel most likely contains maximum physical information. The channel i is found, where the function W_i is at maximum:

$$W_i = \sum_{j=1}^{n} |C_{ij}| \quad j \neq i, i = 1, \ldots n \tag{3}$$

where n is the number of measurement channels.

2.   Repeat step 3 and 4 until all required projection channels are found.
3.   Find the channel that correlates the least with all previous found projection channels. This channel will most likely bring most new information.
4.   If the channel has insignificant correlation with any other channels, it will be discarded since it might be bad, e.g. incorrectly mounted or faulty transducer.

The number of projection channels required can be found by applying the Singular Value Decomposition (SVD) to the spectral densities matrices $G_{yp}(f)$:

$$USV^H = G_{yp}(f) \tag{4}$$

where index y indicate the measurement vector $y(t)$ and p the subset of channels selected as the projection channels. The matrices $G_{yp}(f)$ and S both have dimension $n_y \times n_p$. S is a diagonal matrix consisting of n_p singular values.

By plotting the singular values for all frequencies for every projection channel, all modes will be revealed. The lower singular value curve should approximate a horizontal line over the frequency range of interest, and the other singular value curves should show good mode separation. In that case, the choice of projection channels is optimal as more projection channels will just create new horizontal singular value curves with no additional information. Otherwise more or less projection channels should be used.

Figure 2 shows the aluminum plate example from Figure 1, but without sinusoidal excitation. Too many channels have clearly been selected as projection channels. Figure 3 shows an appropriate choice for the same structure.
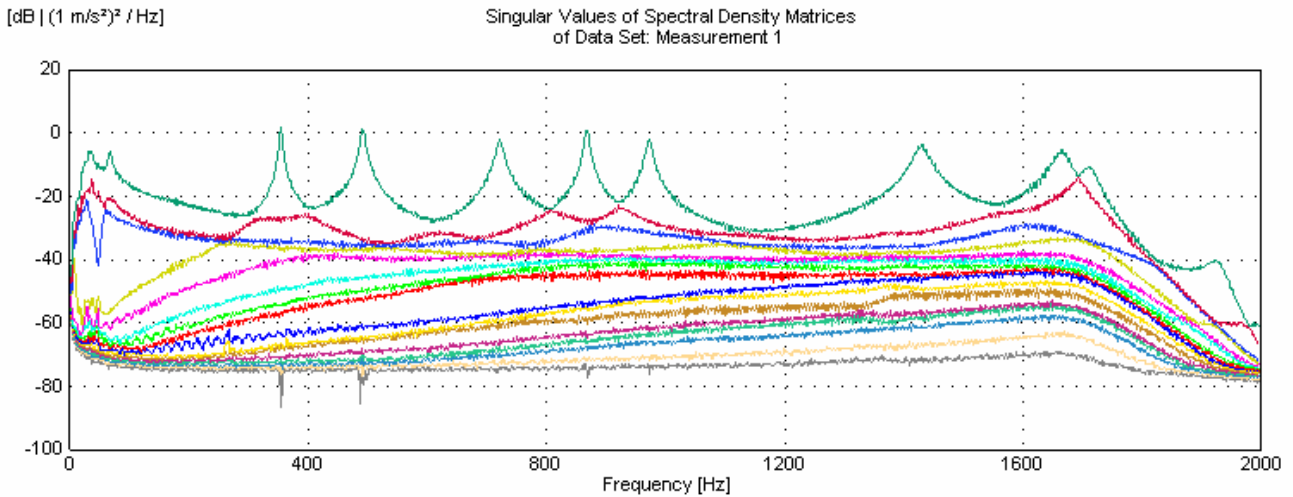

Figure 2. Example with 16 projection channels resulting in 16 singular values per frequency. All the lower singular value curves are basically horizontal indicating a substantial amount of redundant information at all frequencies.
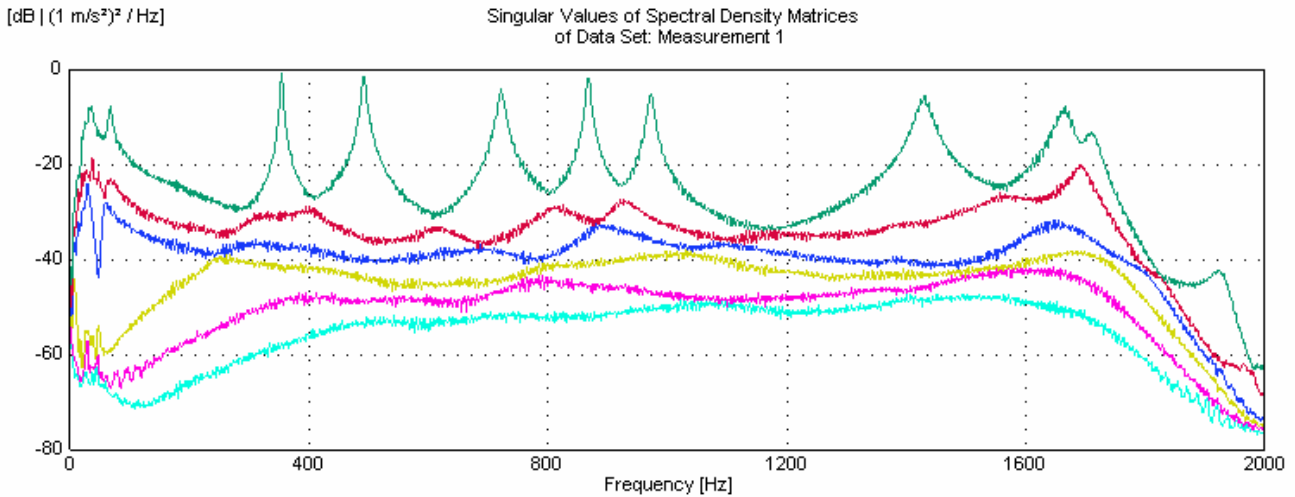
Figure 3. Example with 6 projection channels. The lowest singular value curve is basically horizontal and well attenuated indicating that 6 measurement channels practically contain all the system dynamics.

2.2.2 REDUCING THE NUMBER OF FREQUENCIES

After having reduced the number of channels to be used for the harmonic indicator from all the measurement channels to only the projection channels, the next step is to significantly reduce the number of frequencies to be investigated.

The upper curve in a plot of the singular values of the response spectral density matrix will for a structure excited with purely stochastic excitation have peaks at the natural frequencies indicating high singular values. If all the modes are well-separated, there will only be one dominating mode at each peak and consequently the other curves will be significantly lower and less peaked. In case of closely-coupled modes or repeated roots, peaks will appear on the next lower curves as well. The number of curves with significant peaks equals the number of closely-coupled modes or repeated roots. E.g. two modes at the same frequency will result in two large singular values at that frequency.

In case of strong harmonic excitation of the structure, narrow peaks will be found in multiple of the singular value curves at the harmonic excitation frequency as several modes have been significantly excited at these frequencies. If the harmonic excitation is much weaker than the broad-banded stochastic excitation, the effect of the harmonic excitation becomes negligible and does not affect the modal analysis algorithms.

This phenomenon is illustrated in Figure 1. The natural frequency of the first bending mode appears at 354 Hz and only the first singular value is significant at this frequency. On the other hand, at the deterministic excitation at 374 Hz, 748 Hz (2nd harmonic) and 1496 Hz (4th harmonic), a distinct narrow peak appears in several of the singular value curves.

If an abrupt change happens at the same frequency in at least two singular value curves, then we have detected a potential harmonic component. This potential harmonic component should subsequently be tested using the kurtosis check method described in chapter 2.1. In this way it is possible to significantly reduce the number of frequencies to be checked.

There are several ways to test if there is an abrupt change on a curve, see e.g. Basseville et al. [4]. Here we apply a simple approach based on a median calculation. Given a sequence of positive singular values $S_{i,j}$ of length n_s, where index i is the singular value number and j the discrete frequency index, we construct the following normalized sequence $X_{i,j}$:

$$X_{i,j} = \begin{cases} \log_{10}\left(\dfrac{S_{i,j}}{median\,(S_{i,j-k}\,,...,\,S_{i,j+k})} \right) & ,\, j > k \wedge j < n_s - k \\ 0 & ,\, j \leq k \wedge j \geq n_s - k \end{cases} \tag{5}$$

where k is a small number, say 2-5.

If the median of the values $S_{i,j-k}$ to $S_{i,j+k}$ is equal to the value $S_{i,j}$ then $X_{i,j}$ is 0. Otherwise $X_{i,j}$ will be a non-zero value. Since the sequence is normalized using the median that is robust towards outliers, the result is that $X_{i,j}$ will have significant values at indices corresponding to where the singular value curves have significant but narrow peaks.

The method used here (Fast Kurtosis Check) contains the following steps:
1. For each singular value $S_{i,j}$ calculate the sequences $X_{i,j}$ for i = 1 to n_p and j = 1 to n_s.
2. Calculate the sampled standard deviations of the sequences $X_{i,j}$.
3. Check if some of the values of $X_{i,j}$ exceeds a certain threshold of say 2-3 times the standard deviation of $X_{i,j}$.
4. For those indices j, where more than one of the n_p sequences $X_{i,j}$ exceed the threshold, potential harmonic components have been detected at the j positions.
5. Apply the kurtosis check method described in chapter 2.1 at the j positions.

For the example shown in Figure 1, only the frequencies 28 Hz, 372 Hz, 374 Hz, 376 Hz, 746 Hz, 748 Hz and 1496 Hz were indicated as frequencies for potential harmonic components. Consequently, the method resulted in testing only 7 instead of 1024 frequencies. Using the kurtosis check described in chapter 2.1, only the frequencies 374 Hz, 748 Hz and 1496 Hz were subsequently correctly pointed out as belonging to harmonic components.

3   REMOVING THE INFLUENCE OF THE HARMONIC COMPONENTS

Before describing the new Curve-fitting Frequency Domain Decomposition (CFDD) technique, the original Enhanced Frequency Domain Decomposition (EFDD) technique is briefly explained.

3.1   THE ENHANCED FREQUENCY DOMAIN DECOMPOSITION TECHNIQUE

The original EFDD technique has been described in a series of papers, see e.g. Gade et al. [5]. The EFDD technique rely on a decomposition of the spectrum of the measured response defined as:

$$G_{yy}(f) = H(f)\, G_{xx}(f)\, H^H(f) \tag{6}$$

where $G_{yy}(f)$, $G_{xx}(f)$ and $H(f)$ are the spectra of the measured response, unknown excitation and the Frequency Response Function (FRF), respectively.

The key step in the EFDD technique is to apply a Singular Value Decomposition (SVD) to $G_{yy}(f)$ estimated at the discrete frequencies $f = f_i$:

$$G_{yy}(f_i) = U_i\, S_i\, U_i^H \tag{7}$$

At the natural frequency $f_{j=1}$ the rank of $G_{yy}(f_{j=1})$ is approximately 1 giving:

$$G_{yy}\left(f_{j=1}\right) \sim u_{i1} u_{i1}^H s_{i1} \tag{8}$$

indicating that at the natural frequency the spectrum is approximately equal to the space spanned by the 1st singular vector multiplied by the 1st singular value. As documented in e.g. Brincker et al. [6] the vector u_{i1} is an approximation of the mode shape of the mode with natural frequency $f_{i=1}$.

In the vicinity of the natural frequency it is possible to obtain singular vectors having a high MAC value with u_{i1} which enable us to establish a part of the Single-Degree-Of-Freedom (SDOF) spectral density function for the specific mode. In the following this SDOF spectrum is denoted $S(f)$. In the original implementation of the EFDD technique, this part is transformed to the time domain yielding an auto-correlation function of the SDOF system. From this auto-correlation function the natural frequency is obtained by determining the number of zero-crossing as a function of time using a simple least-squares fit. The damping ratio is obtained from the logarithmic decrement of the auto-correlation function again using a simple least-squares fit.

3.2   THE CURVE-FITTING FREQUENCY DOMAIN DECOMPOSITION TECHNIQUE

The Curve-fitting Frequency Domain Decomposition (CFDD) technique is a novel alternative approach utilizing curve-fitting of $S(f)$ directly in the frequency domain. The main benefit is a more accurate estimation of the natural frequencies and damping ratios both in case of pure stochastic excitation and in the presence of deterministic excitation. The mode shapes are found as in the original EFDD technique as described above.

In Equation (6) the spectral density was defined in terms of the FRF. The FRF for a SDOF system can be expressed in polynomial form as (see Ljung [7]):

$$H(f) = \frac{B_0 + B_1 e^{2\pi jfT} + B_2 e^{4\pi jfT}}{1 + A_1 e^{2\pi jfT} + A_2 e^{4\pi jfT}} \tag{9}$$

where T is the sampling interval.

From the roots of the denominator polynomial the natural frequency and the damping ratio can be extracted directly.

In the following we assume that the unknown excitation $G_{xx}(f)$ in Equation (6) is broad-banded and can be approximated by white noise having a constant spectrum $G_{xx}(f) = G_{xx}$. Consequently, the SDOF spectrum $S(f)$ becomes proportional to the product $H(f)H^H(f)$, indicating that the polynomial order of $S(f)$ is twice the order of $H(f)$.

It would be desirable to avoid having to fit the product $H(f)H^H(f)$, but instead manipulate $S(f)$ so that the fitting can be made directly on $H(f)$ instead. The can be achieved by transforming the full-power spectrum $S(f)$ to a positive half-power spectrum $P(f)$, where $P(f)$ is obtained from $S(f)$ by calculating the respective correlation function obtained by inverse Fourier transformation. Following this step, the negative lags part of the correlation functions is set to zero and $P(f)$ is obtained by Fourier transforming the result back to the frequency domain.

3.2.1 THE CURVE-FITTING ALGORITHM

The first step of the curve-fitting algorithm is to calculate the positive half-power spectrum $P(f)$. Based on this and the formulation of $H(f)$ in Equation (9) we can set up the following relation:

$$(1 + A_1 e^{2\pi jfT} + A_2 e^{4\pi jfT})P(f) = B_0 + B_1 e^{2\pi jfT} + B_2 e^{4\pi jfT} \tag{10}$$

which can be rearranged so the unknown polynomial parameters are isolated:

$$P(f) = \begin{bmatrix} -P(f)e^{2\pi jfT} & -P(f)e^{4\pi jfT} & 1 & e^{2\pi jfT} & e^{4\pi jfT} \end{bmatrix} \begin{bmatrix} A_1 \\ A_2 \\ B_0 \\ B_1 \\ B_2 \end{bmatrix} \tag{11}$$

Given the spectral estimates $P(f_i)$ for all discrete frequencies f_i, $i = 0$ to v, where v is the index of the Nyquist frequency, Equation (11) makes it possible to formulate the following regression problem:

$$A_c\, \theta = B_c \tag{12}$$

where

$$A_c = \begin{bmatrix} -P(f_0)e^{2\pi f_0 T} & -P(f_0)e^{4\pi f_0 T} & 1 & e^{2\pi f_0 T} & e^{4\pi f_0 T} \\ -P(f_1)e^{2\pi f_1 T} & -P(f_1)e^{4\pi f_1 T} & 1 & e^{2\pi f_1 T} & e^{4\pi f_1 T} \\ . & . & . & . & . \\ . & . & . & . & . \\ -P(f_v)e^{2\pi f_v T} & -P(f_v)e^{4\pi f_v T} & 1 & e^{2\pi f_v T} & e^{4\pi f_v T} \end{bmatrix}, \quad B_c = \begin{bmatrix} P(f_0) \\ P(f_1) \\ . \\ . \\ P(f_v) \end{bmatrix}, \quad \theta = \begin{bmatrix} A_1 \\ A_2 \\ B_0 \\ B_1 \\ B_2 \end{bmatrix} \tag{13}$$

In order to assure that the parameters of θ will be estimated as real valued parameters as they are defined, the complex relation in Equation (12) is reformulated to a regression problem of double size:

$$\begin{bmatrix} \mathrm{Re}(A_c) \\ \mathrm{Im}(A_c) \end{bmatrix} \theta = \begin{bmatrix} \mathrm{Re}(B_c) \\ \mathrm{Im}(B_c) \end{bmatrix} \tag{14}$$

and a solution is found as:

$$\hat{\theta} = \begin{bmatrix} \mathrm{Re}(A_c) \\ \mathrm{Im}(A_c) \end{bmatrix}^{-1} \begin{bmatrix} \mathrm{Re}(B_c) \\ \mathrm{Im}(B_c) \end{bmatrix} \tag{15}$$

The matrix inversion in Equation (15) is a pseudo-inversion since the matrix has much more rows than columns.

3.2.2 THE CURVE-FITTING ALGORITHM IN THE PRESENCE OF HARMONIC COMPONENTS

When the curve-fitting algorithm is applied on responses containing harmonic components, the harmonic components first have to be removed. In Jacobsen et al. [2], an approach was used where the harmonic components were removed by linear interpolation in the SVD plot. This is shown for the aluminum plate structure in Figure 4.
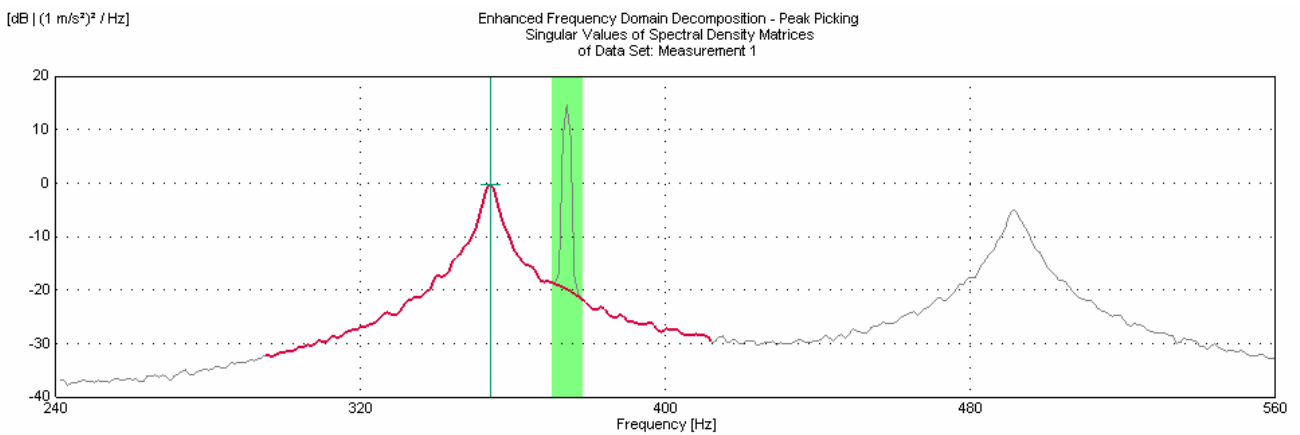

Figure 4. Removal of harmonic component in the SVD plot using linear interpolation. Structural mode at 354 Hz. Harmonic component at 374 Hz.

The method gave good results but the accuracy could be improved when a harmonic component was located exactly at or close to the natural frequency of a structural mode. In these cases the estimation of the natural frequency would be biased and the damping ratio would be overestimated – the peak of the SDOF function was slightly cut off due to the linear interpolation.

When subsequently using curve-fitting the limitation of the linear interpolation is less critical. Consequently the linear interpolation method has been applied in the initial implementation of the CFDD technique. However, a least-squares fit approach is currently being investigated, where extrapolation is made from singular values at both sides of the harmonic component.

Figure 5 shows for the aluminum plate example the CFDD curve-fitter on the interpolated SDOF function.
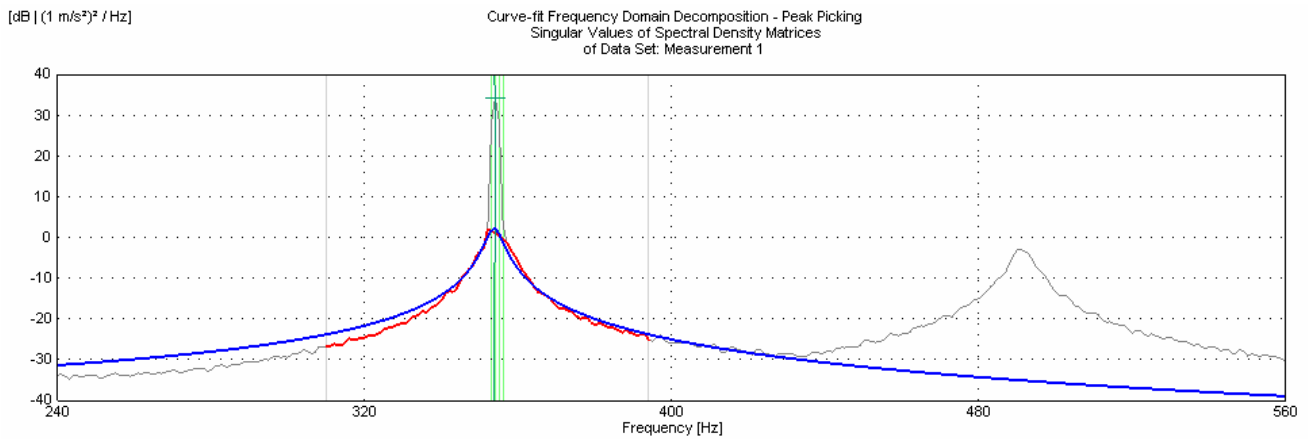

Figure 5. Removal of harmonic component in the SVD plot using linear interpolation (red graph) and subsequent using the CFFD curve-fitter (blue graph). Structural mode and harmonic component both at 354 Hz.

4   APPLICATIONS OF THE CFDD TECHNIQUE

The CFFD technique is, of course, advantageous both in the case of pure stochastic excitation and when harmonic components are present. However, in the latter case the benefits will be more significant. The loading forces of mechanical engineering structures like aircraft, helicopters, vehicles, ships, submarines, engines, generators, turbines, compressors, white goods, disk drives, power tools etc. are often quite complex. They are typically a combination of harmonic components originating from the rotating and reciprocating parts and broadband excitation originating from either self-generated vibrations from, for example, bearings and combustions or from ambient excitations like air turbulence and road vibrations.

Though civil engineering structures like buildings, towers, bridges and offshore structures are mainly loaded by ambient forces like wind, waves, traffic or seismic micro-tremors, they can also have significant loading with harmonic components from, for example, ventilation systems, turbines and generators.

In the following two examples are shown - a ship structure and a gravity dam.

4.1   APPLICATION EXAMPLE – SHIP STRUCTURE

In this example, the measurements described in Rosenow et al. [8] are analyzed with the Fast Kurtosis Check method and the CFDD technique. The measurements were done by Sven-Erik Rosenow, Santiago Uhlenbrock and Günther Schlottmann from University of Rostock, Germany.

The structure, which is shown in Figure 6, is a roll-on roll-off ship from Flensburg shipyard.

Shipyard:
Flensburger Schiffbaugesellschaft
Length over all: 199,8 m
Ship speed: 22,5 kn

Main engine:
9L 60 MC-C (MAN B&W, 9 cylinder)
Power: 20 070 kW
Nominal rotation speed: 123 rpm
Working process: two-stroke

Propeller:
4-bladed with controllable pitch

Figure 6. Investigated object, roll-on roll-off ship at the Flensburg shipyard and ship data.

An in-operation test of the ship was carried out in a single data set using 16 channels. The measurement time was 5400 s (90 min) and with a sampling frequency of 128 Hz. The number of projection channels was set to 6. The harmonic detection described in Chapter 2.2 was applied using $k = 2$ in Equation (5). The threshold used in step 3 of the algorithm was set to 2 times the standard deviation of the sequence $X_{i,j}$.

In Figure 7 the results of the harmonic detection is shown. The main engine introduces excitation forces into the ship structure at all frequencies that are whole multiples of its rotational frequency (two-stroke engine). In this specific test, the rotational frequency was 2.05 Hz. From the propeller, main excitation forces are transmitted into the ship in form of pressure pulses acting on the ship's hull. The propeller blade frequencies are multiples of 8.20 Hz (4-bladed propeller). All harmonic components at 2.05 Hz interval have clearly been detected.
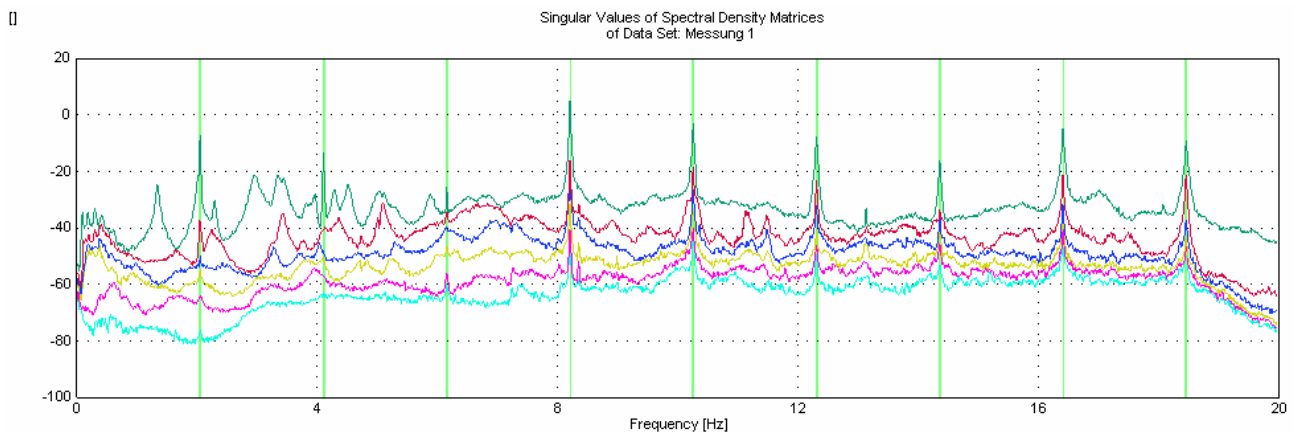

Figure 7. Harmonic components with 2.05 Hz interval are clearly detected.

The first harmonic component resulting from the first excitation order of the main engine is very close to the second structural mode. In Figure 8, the CFDD curve-fitter is shown on the second structural mode after prior linear interpolation in the SDOF function. The harmonic component is clearly eliminated and the second structural mode properly extracted.
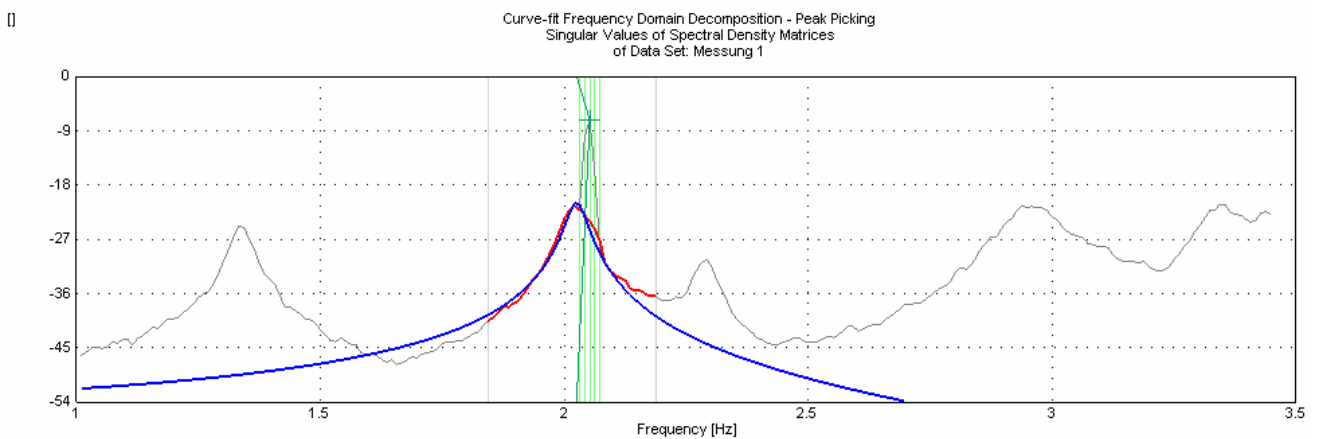
Figure 8. Removal of harmonic component in the SVD plot using linear interpolation (red graph) and subsequent using the CFFD curve-fitter (blue graph). Structural mode at 2.03 Hz. Harmonic component at 2.05 Hz.

4.2   APPLICATION EXAMPLE – GRAVITY DAM

This example is from Andersen et al. [3]. The measurements were done by Carlos Ventura, University of British Columbia, Canada.

The structure, which is shown in Figure 9, is a gravity dam of dimensions 58 m high and 130 m long built in 1930.
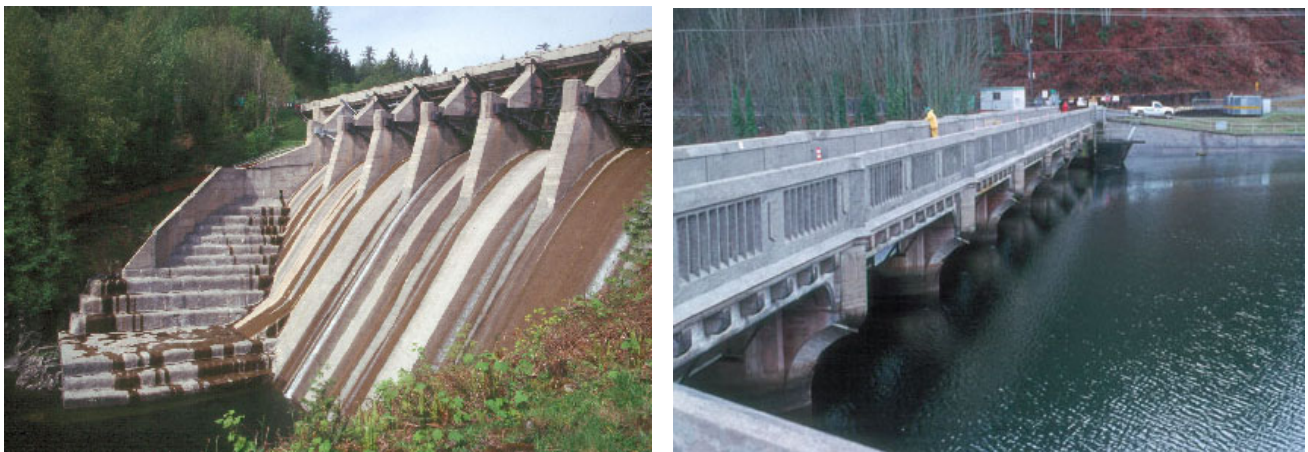

Figure 9. The gravity dam seen from low (left) and high (right) water levels.

An ambient vibration test was conducted in 20 data sets each with 8 channels. 3 reference DOFs were used. The measurement time was 819 s and with a sampling frequency of 80 Hz. As one of the transducers was bad in one of the data sets, the number of projection channels used in the analysis was set to 7. The harmonic detection described in Chapter 2.2 was applied using $k = 2$ in Equation (5). The threshold used in step 3 of the algorithm was set to 2 times the standard deviation of the sequence $X_{i,j}$.

In Figure 10 the results of the harmonic detection is shown. Due to the turbines running, the measurements are affected by harmonic components at every 2 Hz. All harmonic components at 2 Hz interval have been detected. The algorithm has incorrectly detected two harmonic components at 19.5 Hz and 39 Hz, respectively. Taking the scatter of the SVD spectrum from the poor signal-to-noise ratio into account, it is a quite satisfactory result.
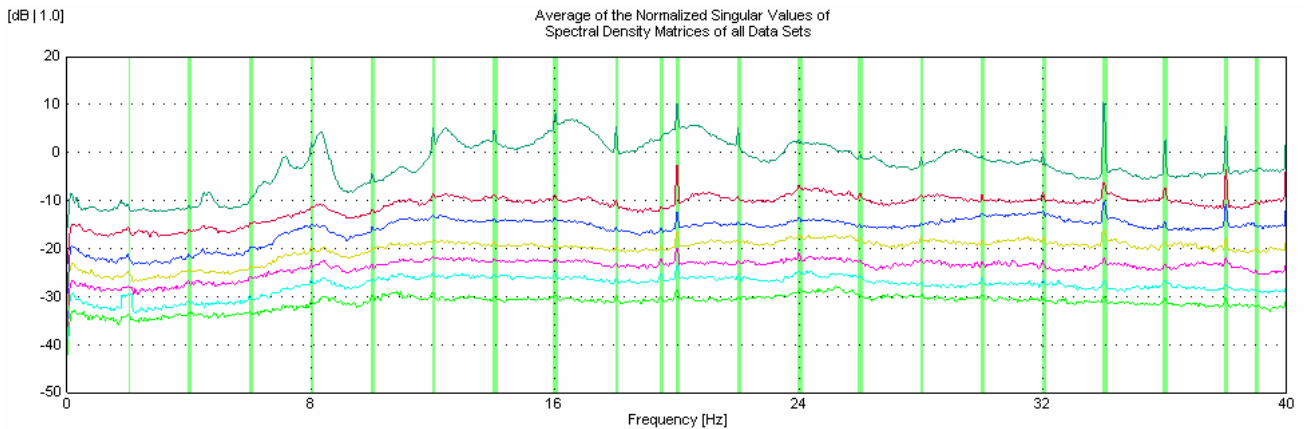
Figure 10. Harmonic components with 2 Hz interval are clearly detected. The algorithm has incorrectly detected harmonic components at 19.5 Hz and 39 Hz due to poor signal-to-noise ratio.

5.   CONCLUSIONS AND FUTURE WORK

The presence of dominant harmonic components in the measured responses is unavoidable in many applications of Operational Modal Analysis. The consequences can be quite drastic and can result in significantly biasing of the modal parameters obtained or even prohibit the extraction of the structural modes.

This paper has described a new method based on the original EFDD technique, where the harmonic components are identified using a Fast Kurtosis Check method and then removed by first performing a linear interpolation across the harmonic components in the SDOF function and secondly applying a curve-fitting using the novel CFDD technique. The method has been demonstrated on measurements from a ship structure and a gravity dam.

This new combined approach offers some distinct benefits:
• Robust method – Harmonic components are clearly identified and their effect can be eliminated even in the case of a harmonic component located exactly at a structural mode.
• No prior knowledge required – For example about the number of harmonic components and their frequencies.
• Easy-to-use – Automated method based on the CFDD technique.
• Fast – Based on computational efficient algorithms using Fast Kurtosis Checking.

Future work will include examination of a least-squares fit extrapolation instead of the linear interpolation in the SDOF functions, where the extrapolation is made from singular values at both sides of a harmonic component. Finally, a new method for eliminating harmonic components before using the Stochastic Subspace Identification (SSI) techniques will be worked on.

REFERENCES

[1]   Jacobsen, N-J
        Separating Structural Modes and Harmonic Components in Operational Modal Analysis
        IMAC XXIV Conference, 2006

[2]   Jacobsen, N-J; Andersen, P; Brincker, R
        Eliminating the Influence of Harmonic Components in Operational Modal Analysis
        IMAC XXV Conference, 2007

[3]   Andersen, P; Brincker, R; Venture, C; Cantieni, R
        Estimating Modal Parameters of Civil Engineering Structures subject to Ambient and Harmonic Excitation
        EVACES´07 Conference, 2007

[4]   Basseville, M; Nikiforov, I
        Detection of Abrupt Changes - Theory and Applications
        Prentice Hall, ISBN 0-13-126780-9, 1993

[5]   Gade, S; Møller, N; Herlufsen, H; Konstantin-Hansen, H
        Frequency Domain Techniques for Operational Modal Analysis
        1st IOMAC Conference, 2005

[6]   Brincker, R; Zhang, L; Andersen, P
        Output-Only Modal Analysis by Frequency Domain Decomposition
        ISMA25 Conference, 2000

[7]   Ljung, L
        System Identification – Theory for the User, 2nd Edition
        Prentice Hall, Upper Saddle River, N.J.,1999

[8]   Rosenow, S-E; Uhlenbrock, S; Schlottmann, G
        Parameter Extraction of Ship Structures in Presence of Stochastic and Harmonic Excitations
        2nd IOMAC Conference, 2007